

Selecting of Slotted AFPM Motors with High Torque Density for Electric Vehicles

S.Asghar Gholamian, M. Ardebili, K. Abbaszadeh and Seyed Akbar Gholamian

Abstract— Double-sided axial flux PM motors (AFPM) are the most promising and widely used types. There are two topologies for slotted double-sided AFPM motors. Selecting an AFPM motors with high torque density is an important parameter in applications. So, comparison of torque density between different topologies of double-sided AFPM motors seems to be necessary.

In this paper, the sizing equations of axial flux slotted one-stator-two-rotor (TORUS) and two-stator-one-rotor (AFIR) type PM motors is presented and comparison of the TORUS and AFIR topologies in terms of torque density is illustrated. Field analysis of both Topologies of slotted motors is investigated using Finite Element method (FEM) software. Finally a high torque double-sided slotted AFPM motor is introduced in the paper.

Index Terms— axial flux PM motors (AFPM), torque density, electrical loading and Finite Element method (FEM).

1 INTRODUCTION

In conventional machines, the air gap flux density has normally radial direction. In AFPMs, the air gap flux density presents mainly axial direction. In general, AFPMs exhibit an axial length much smaller than the length of a conventional motor of the same rating [1-3].

AFPM motors are particularly suitable for electrical vehicles and industrial equipment. The large diameter rotor with its high moment of inertia can be utilized as a flywheel. These machines are ideal for low speed applications, as for example, electromechanical traction drives hoists. Traction electric motors for EVs should meet high power density, high torque at low speed for starting and climbing, high speed at low torque for cruising, high efficiency over wide speed and torque ranges [1,6].

Selecting of double-sided AFPM motors with high torque density is an important parameter, especially in electrical vehicle applications. So, comparison of torque density between different topologies of double-sided AFPM motors seems to be necessary [3].

The AFPM machine, also called the disc-type machine, is an attractive alternative to the cylindrical RFPM machine due to its pancake shape, high efficiency, compact Construction and high power density [1,3].

There are two topologies for slotted double-sided AFPM motors. These topologies are axial flux slotted one-stator-two-rotor (TORUS) and two-stator-one-rotor (AFIR) type PM motors. Two AFPM motors and their acronyms are selected TORUS-S (Axial flux slotted external rotor internal stator PM stator) and AFIR-S (Axial flux slotted internal rotor external stator PM motor) for detailed analysis. The stator cores of the machine is formed by tape wound core with a lap and short-pitched polyphase AC winding located in punched stator slots. The rotor structure is formed by the axially magnetized NdFeB magnets [4,5].

The topologies used in the study are illustrated in Fig.1.

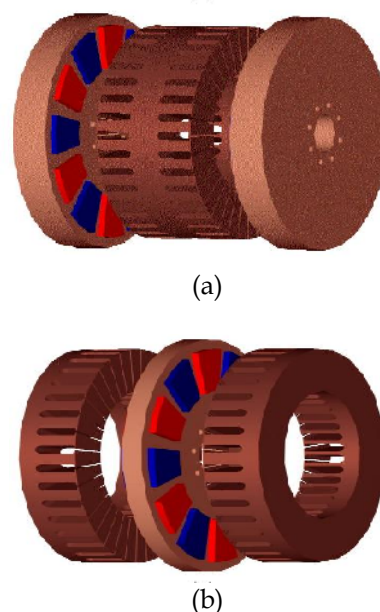


Fig.1. Axial flux slotted (a) one-stator-two-rotor TORUS-S type (b) two-stator-one-rotor AFIR-S type

- S. Asghar Gholamiann, Faculty of Electrical Engineering, Babol University of Technology, Babol, Iran, Email: gholamian@nit.ac.ir
- M. Ardebili, Electrical Engineering Department of K.N. Toosi University of Technology, Tehran, Iran, Email: ardebili@eetd.kntu.ac.ir
- K. abbaszadeh, Electrical Engineering Department of K.N. Toosi University of Technology, Tehran, Iran, Email: abbaszadeh@eetd.kntu.ac.ir
- Seyed Akbar Gholamian, Department of Industrial Engineering, Payame Noor University, Babol, Iran, ag1358@gmail.com

Flux directions of both AFIR and TORUS slotted topologies at the average diameter in 2D are also shown in Fig. 2a and 2b.

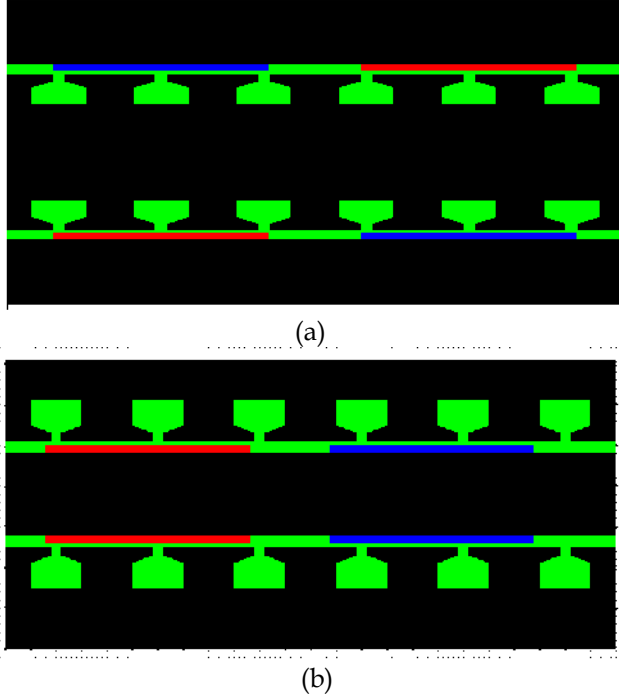


Fig.2. One pole pair of the (a) TORUS-S (b) AFIR-S

Increasing the air gap length, maximum torque density will change in AFPM motors. These changes are not the same in different topologies. Maximum torque density of TORUS-S is higher than AFIR-S in large air gap length.

In Section2, the generalized sizing approach for TORUS-S and AFIR-S types PM motors is briefly discussed. Then, some results of comparisons of the TORUS-S and AFIR-S topologies in terms of torque density are illustrated in Section3. In Section 4, Field analyses of both Topologies of slotted motors are investigated using Finite Element method (FEM) by MAXWELL10 software. In Section 5, effect of electrical loading and current density are illustrated. The conclusions are given in Section6.

2. Sizing equations of AFPM Motors

In general, if stator leakage inductance and resistance are neglected, the output power for any electrical machine can be expressed as

$$P_{out} = \eta \frac{m}{T} \int_0^T e(t) \cdot i(t) dt = m K_p \eta E_{pk} I_{pk} \quad (1)$$

where

$e(t)$ and E_{pk} are phase air gap EMF and its peak value, $i(t)$ and I_{pk} are phase current and the peak phase cur-

rent, η is machine efficiency, m is number of phases of the machine and T is period of one cycle of the EMF[4,5,7].

The quantity K_p is termed the electrical power waveform factor and defined as

$$K_p = \frac{1}{T} \int_0^T \frac{e(t) \times i(t)}{E_{pk} \times I_{pk}} dt = \frac{1}{T} \int_0^T f_e(t) \cdot f_i(t) dt \quad (2)$$

where

$f_e(t) = e(t)/E_{pk}$ and $f_i(t) = i(t)/I_{pk}$ are the expressions for the normalized EMF and current waveforms. In order to indicate the effect of the current waveform, a definition for current waveform factor, K_i , is also useful,

$$K_i = \frac{I_{pk}}{I_{rms}} = \left[\frac{1}{T} \int_0^T \left(\frac{i(t)}{I_{pk}} \right)^2 dt \right]^{-0.5} \quad (3)$$

where

I_{rms} is the rms value of the phase current. The peak value of the phase air gap EMF for AFPM in (1) is given by:

$$E_{pk} = K_e N_{ph} B_g \cdot \frac{f}{p} \cdot (1 - \lambda^2) D_o^2 \quad (4)$$

where

K_e is the EMF factor which incorporates the winding distribution factor K_w and the per unit portion of the total air gap area spanned by the salient poles of the machine (if any), N_{ph} is the number of turn per phase, B_g is the flux density in the air gap, f is the converter frequency, p is the machine pole pairs, λ is the diameter ratio for AFPM defined as D_i/D_o , D_o is the diameter of the machine outer surface, D_i is the diameter of the machine inner surface. The peak phase current in (1) is given by:

$$I_{pk} = A \pi K_i \frac{1 + \lambda}{2} \cdot \frac{D_o}{2m_1 N_{ph}} \quad (5)$$

where

m_1 is number of phases of each stator and A is the electrical loading.

Combining (1) through (5), the general purpose sizing equations take the following form for AFPM.

$$P_{out} = \frac{m}{m_1} \frac{\pi}{2} K_e K_p K_i A B_g \eta \frac{f}{p} (1 - \lambda^2) \left(\frac{1 + \lambda}{2} \right) D_o^3 \quad (6)$$

The machine torque density for the total volume can be defined as

$$T_{den} = \frac{P_{out}}{\omega_m \frac{\pi}{4} D_{tot}^2 L_{tot}} \quad (7)$$

where

ω_m is the rotor angular speed, D_{tot} is the total machine outer diameter including the stack outer diameter and the protrusion of the end winding from the iron stack

in the radial direction, L_{tot} is the total length of the machine including the stack length and the protrusion of the end winding from the iron stack in the axial direction [4,5,7].

1.1. Sizing Equations for the TORUS-S

The generalized sizing equation approach can easily be applied to axial flux permanent magnet TORUS type motor [5].

The outer surface diameter D_o can be written as

$$D_o = \left(P_{out} / \frac{\pi m}{2m_1} K_e K_p K_i A B_g \eta \frac{f}{p} (1 - \lambda^2) \left(\frac{1 + \lambda}{2} \right) \right)^{1/3} \quad (8)$$

The machine total outer diameter D_{tot} for the TORUS-S motor is given by

$$D_{tot} = D_o + 2W_{cu} \quad (9)$$

where

W_{cu} is the protrusion of the end winding from the iron stack in the radial direction. For the back-to-back wrapped winding, protrusions exist toward the axis of the machine as well as towards the outsides and can be calculated as

$$W_{cu} = \frac{D_i - \sqrt{D_i^2 - \left(\frac{2AD_g}{K_{cu} J_s} \right)^2}}{2} \quad (10)$$

where

D_g is the average diameter of the machine, J_s is the current density and K_{cu} is the copper fill factor.

Note for the slotted topology machines the depth of the stator slot for slotted motors is $L_{ss} = W_{cu}$.

The axial length of the machine L_e is given by

$$L_e = L_s + 2L_r + 2g \quad (11)$$

where

L_s is axial length of the stator, L_r is axial length of the rotor and g is the air gap length. The axial length of the stator L_s is

$$L_s = L_{cs} + 2L_{ss} \quad (12)$$

The axial length of the stator core L_{cs} can be written as

$$L_{cs} = \frac{B_g \pi \alpha_p D_o (1 + \lambda)}{4p B_{cs}} \quad (13)$$

where

B_{cs} is the flux density in the stator core and α_p is the ratio of average air gap flux density to peak air gap flux density. The axial length of rotor L_r becomes

$$L_r = L_{cr} + L_{PM} \quad (14)$$

Also, the axial length of the rotor core L_{cr} is

$$L_{cr} = \frac{B_u \pi D_o (1 + \lambda)}{8p B_{cr}} \quad (15)$$

where

B_{cr} is the flux density in the rotor disc core, and B_u is

the attainable flux density on the surface of the PM. The PM length L_{PM} can be calculated as

$$L_{PM} = \frac{\mu_r B_g}{B_r - \left(\frac{K_f}{K_d} B_g \right)} K_c g \quad (16)$$

where

μ_r is the recoil relative permeability of the magnet, B_r is the residual flux density of the PM material, K_d is the leakage flux factor, K_c is the Carter factor, $K_f = B_{gpk}/B_g$ is the peak value corrected factor of air gap flux density in radial direction of the AFPM motor. These factors can be obtained using FEM analysis [5].

1.2. Sizing Equations for the AFIR-S

The concept of Double-sided Axial Flux two-stator-one-rotor (AFIR) type PM motors was presented in [4].

The outer surface diameter D_o is obtained from (6).

$$D_o = \left(2P_{out} / \frac{\pi m}{2m_1} K_e K_p K_i A B_g \eta \frac{f}{p} (1 - \lambda^2) \left(\frac{1 + \lambda}{2} \right) \right)^{1/3} \quad (17)$$

The machine total outer diameter D_{tot} for the AFIR type machines is given as

$$D_{tot} = D_o + 2W_{cu} \quad (18)$$

where

W_{cu} is the protrusion of the end winding from the iron stack in the radial direction and can be calculated as

$$W_{cu} = \frac{(0.46 - 0.62)D_o}{p} \quad (19)$$

The axial length of the machine L_e is

$$L_e = L_r + 2L_s + 2g \quad (20)$$

where

L_s is axial length of the stator, L_r is axial length of the rotor and g is the air gap length. The axial length of a stator L_s is

$$L_s = L_{cs} + d_{ss} \quad (21)$$

where

L_{cs} is the axial length of the stator core, and the depth of the stator slot for slotted machines d_{ss} is

$$d_{ss} = \frac{D_i - \sqrt{D_i^2 - \left(\frac{2AD_g}{\alpha_s K_{cu} J_s} \right)^2}}{2} \quad (22)$$

where

α_s is the ratio of stator teeth portion to the stator pole.

The axial length of the stator core L_{cs} can be written as

$$L_{cs} = \frac{B_g \pi \alpha_p D_o (1 + \lambda)}{8p B_{cr}} \quad (23)$$

Since there is no rotor core in rotor PM topologies, the axial length of rotor L_r is

$$L_r = L_{PM} \quad (24)$$

The PM length L_{PM} can be calculated as

$$L_{PM} = \frac{2\mu_r B_g}{B_r - \left(\frac{K_f}{K_d} B_g\right)} K_c g \quad (24)$$

3. Comparison of slotted TORUS and AFIR

Comparison of two different Double-sided axial flux slotted PM motors in terms of torque density is accomplished for 10KW output power, 4 poles and 60Hz drive. In this comparison, other constant parameters of motors are tabulated in table1.

Table1. Constant parameters of motors in comparison

Number of phases	3
Slot fill factor	0.8
Pole arc ratio	0.75
Slot per Pole per Phase	1
flux density in stator	1.5 T
flux density in rotor	1.5 T
Efficiency	90%
Residual flux density of PM	1.1 T

In AFPM motors, the air gap flux density and diameter ratio are the two important design parameters which have significant effect on the motor characteristics. Therefore, in order to optimize the motor performance, the diameter ratio and the air gap flux density must be chosen carefully. Fig.3 shows the torque density variation as a function of air gap flux density and the diameter ratio for the AFIR-S and TORUS-S motors.

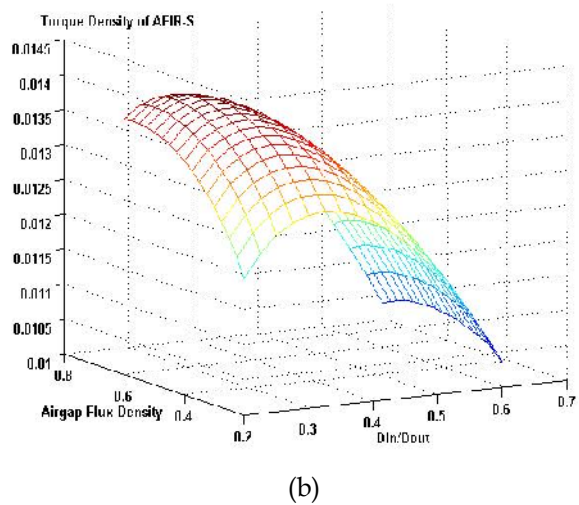
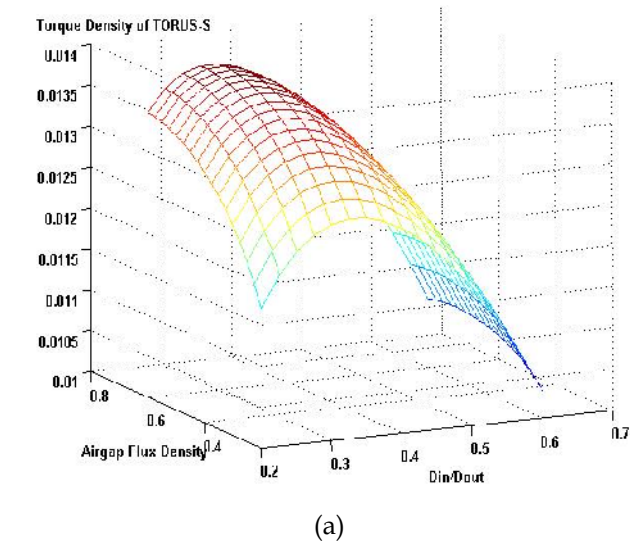


Fig.3. Torque density vs. air gap flux density and diameter ratio for A=30000 (A/m), g=1 (mm), Js=9000000 (A/m²) a) TORUS-S b) AFIR-S

As can be seen from Fig.3b, the maximum torque density occurs at Bg=0.51 (T) and λ = 0.27. In various air gap length, the maximum torque density occurs in different Bg and λ.

Table2 shows maximum torque density with corresponding Bg and λ.

Table2. Maximum torque density with corresponding Bg and λ

Type	g (mm)	Bg (T)	λ	Maximum torque density (N.m/cm³)
TORUS-S	1	0.56	0.3	0.014
	1.5	0.57	0.3	0.0137
	2	0.58	0.27	0.0134
AFIR-S	1	0.51	0.27	0.014
	1.5	0.52	0.27	0.0136
	2	0.53	0.28	0.0133

Fig.4 shows the maximum torque density variation as a function of air gap length for the AFIR-S and TORUS-S motors for A=30000 (A/m), Js=9000000 (A/m²).

In special air gap length (this air gap length is called G_T) maximum torque density of AFIR-S and TORUS-S motors will be the same. Considering Fig.4, it can be concluded that in large air gap length, slotted TORUS motor has high power density.

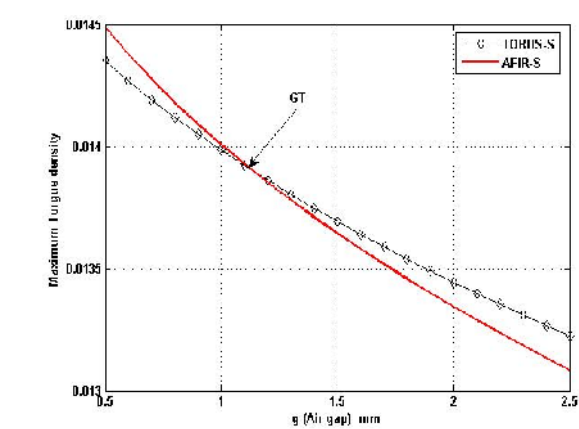


Fig.4. Maximum torque density AFIR-S and TORUS-S vs. air gap length

4. 2D Finite element method Analysis of field

In order to analyze the magnetic circuit and power density, 2D Finite Element Analysis was used for both TORUS-S and AFIR-S type motors [2]. The purpose of the FEM is to get the overall picture of the saturation levels in various parts of the machine, to compare the flux densities obtained from FEM and sizing analysis.

4.1. FEM of the AFIR-S Motor

The motor parameters and important design dimensions used for the AFIR-S model are shown in Table 3. Fig.5 shows the flux distribution over one pole pair using FEM. Fig.6 shows the air gap Flux density over one pole at the average diameter (Dg) using FEM. This curve shows that the flux density on the edge of the Slots is about 13% lower than the flux density on the center of the PM because of the magnet leakage flux.

Table3. Parameters and dimensions of slotted AFIR-S motor

Air gap length	1 mm
Slot depth	9 mm
Pole-arc-ratio	0.75
Axial length of stator core	16 mm
Axial length of rotor core	40 mm
Axial length of PM	2 mm
Outer diameter	367 mm
Inner diameter	95.5 mm

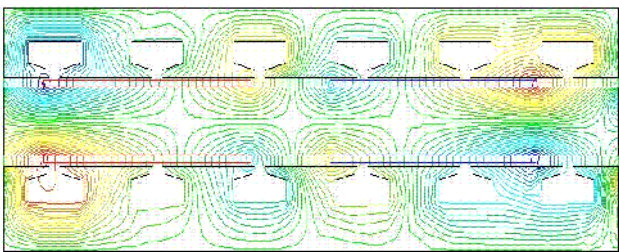


Fig.5. flux distribution over one pole pair for AFIR-S

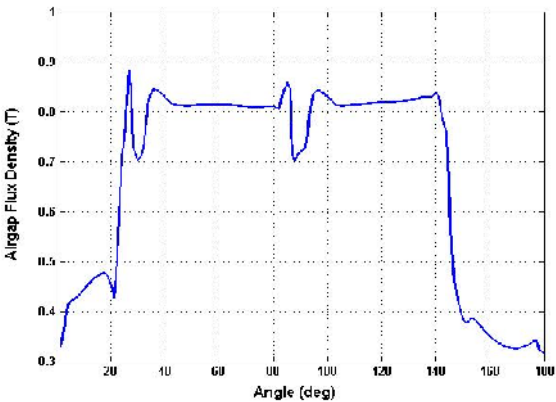


Fig.6. Air gap flux density over one pole for AFIR-S

A flux density comparison between the FEM results and sizing analysis results on various parts of the slotted AFIR motor at no load is tabulated in Table 4. The comparison table shows that the FEM results are consistent with the results obtained from the sizing analysis.

Table4. Flux density comparison of slotless AFIR-S motor

	Rotor	Air gap		Stator
	B _{cr}	B _{max}	B _{avg}	B _{cs}
FEM	1.5	0.82	0.55	1.45
Sizing Eq.	1.5 T	0.8	0.53	1.5

4.2. FEM of the TORUS-S Motor

The parameters and optimized TORUS-S motor dimensions used in the design which are calculated using sizing equations are shown in Table 5.

Table5. Parameters and dimensions of slotted TORUS-S motor.

Air gap length	1 mm
Slot depth	10 mm
Pole-arc-ratio	0.75
Axial length of stator core	42 mm
Axial length of rotor core	25 mm
Axial length of PM	2 mm
Outer diameter	356 mm
Inner diameter	103 mm

Fig.7 shows the flux distribution over one pole pair using FEM. The air gap flux density at the average diameter (D_g) over one pole using FEM was obtained and is shown in Fig.8.

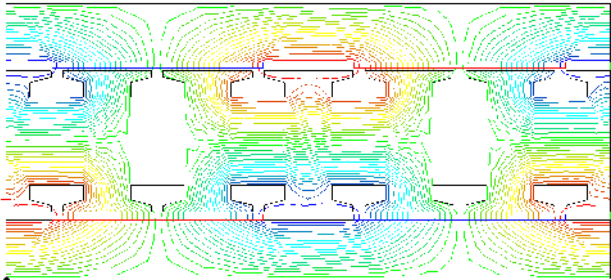


Fig.7. flux distribution over one pole pair for TORUS-S

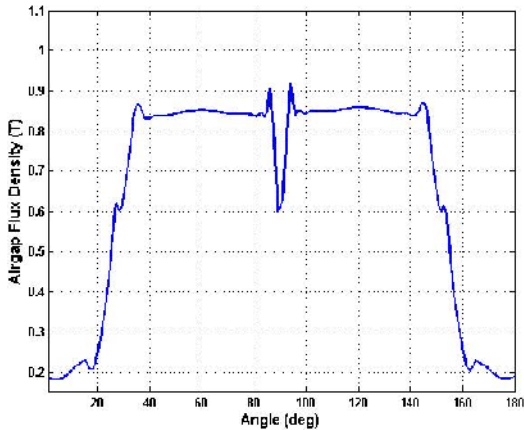


Fig.8. Air gap flux density over one pole for TORUS-S

A comparison of the flux densities between the FEM results and sizing analysis results for different parts of the machine at no load is tabulated in Table 6.

Table6. Flux density comparison of slotless TORUS-S motor

	Rotor	Air gap		Stator
	B_{cr}	B_{max}	B_{avg}	B_{cs}
FEM	1.52	0.85	0.6	1.44
Sizing Eq.	1.5 T	0.8	0.58	1.5

From the no load flux density plots, it is seen that the results are again consistent with the results obtained from the sizing analysis, the maximum flux density values on the rotor and stator came out almost the same. Also, the maximum and average air gap flux densities obtained from the FEM and sizing analysis agree well.

5. Effect of electrical loading and current density

The considerable point is that the value of G_T will vary when the electrical loading 'A' changes.

Fig.9 shows the variation of the maximum torque density as a function of air gap length in $A=25000$ (A/m) for the AFIR-S and TORUS-S motors.

Fig.10 shows the variation of the maximum torque density as a function of air gap length in $A=35000$ (A/m) for the AFIR-S and TORUS-S motors also.

According to fig.10 it can be concluded that point G_T is shifted to larger air gaps and this means that in smaller air gaps AFIR-S motor has higher maximum torque density. According to figure 5 it can be concluded that point G_T is shifted to smaller air gaps and this means that in higher air gaps TORUS-S motor has higher maximum torque density. Other value of G_T for various A is tabulated in table 7.

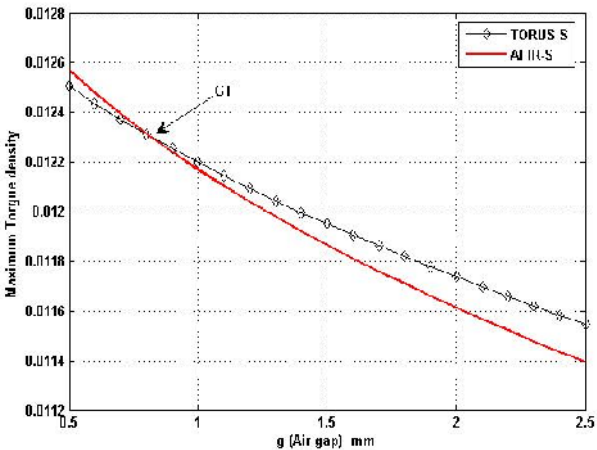


Fig.9. Maximum torque density AFIR-S and TORUS-S vs. air gap length for $A=25000$ (A/m)

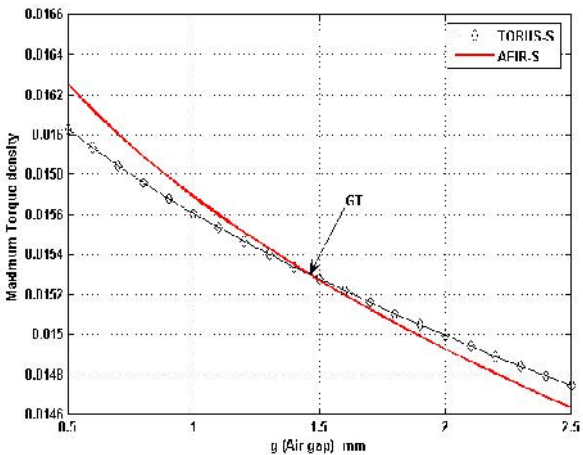


Fig.10. Maximum torque density AFIR-S and TORUS-S vs. air gap length for $A=35000$ (A/m)

Table7. Other value of GT for Various A

A (A/m)	G _T (mm)
15000	0.43
20000	0.58
25000	0.81
30000	1.12
35000	1.46
40000	1.93

6. CONCLUSION

Selecting an AFPM motors with higher torque density is an important parameter in applications. The main goal of this paper has been introduce to double-Sided Axial Flux Slotted PM Motors with maximum torque density. There are two topologies for slotted double-sided AFPM motors.

The maximum torque density is changed by different value of the air gap and electrical loading. TORUS-S topology has high torque density in low electrical loading. But, AFIR-S topology has high torque density in high electrical loading.

A flux density comparison between the various parts of the slotted AFIR-S and TORUS-S motors obtained from the FEM and sizing analysis at no load agree well.

REFERENCES

- [1] S.A. Gholamian, M. Ardebil, K. Abbaszadeh and S. Mahmodi charati; "Optimum Design of 1kW Axial Flux Permanent Magnet Slotted TORUS Motor", European Journal of Scientific Research, ISSN 1450-216X, Vol.21 No.3 (2008), pp.488-499.
- [2] S. Asghar Gholamian, M. Ardebili. K. Abbaszadeh, "Selecting and Construction of High Power Density Double-Sided Axial Flux Slotted Permanent Magnet Motors for Electric Vehicles", IREE, Vol. 4. n. 3, pp. 477-484, 2009.
- [3] Jacek F. Gieras, Rong-Jie Wang and Maarten J. Kamper, "Axial Flux Permanent Magnet Brushless Machines", Publisher: Springer; 1 edition (January 4, 2005).

[4] Aydin, M.; Huang, S.; Lipo, T.A.; "Optimum design and 3D finite element analysis of nonslotted and slotted internal rotor type axial flux PM disc Machines", Power Engineering Society Summer Meeting, 2001. IEEE Volume 3, 15-19 July 2001 Page(s):1409 - 1416 vol.3.

[5] Aydin, M.; Surong Huang; Lipo, T.A.; "Design and 3D electromagnetic field analysis of non-slotted and slotted TORUS type axial flux surface mounted permanent magnet disc machines", Electric Machines and Drives Conference, 2001. IEMDC 2001. IEEE International2001 Page(s): 645 - 651.

[6] Caricchi, F.; Capponi, F.G.; Crescimbeni, F.; Solero, L.; "Experimental study on reducing cogging torque and core power loss in axial-flux permanent-magnet machines with slotted winding", Industry Applications Conference, 2002. 37th IAS Annual Meeting. Conference Record of the Volume 2, 13-18 Oct. 2002 Page(s):1295 - 1302 vol.2.

[7] S. Huang, J. Luo, F. Leonardi and T. A. Lipo, "A Comparison of Power Density for Axial Flux Machines Based on the General Purpose Sizing Equation", IEEE Trans. on Energy Conversion, Vol.14, No.2 June 1999, pp. 185-192.